

Magnetoelastic Force Sensor Using Amorphous Alloy

D. Son and C. S. Kim

Korea Standards Research Institute, P.O.Box 3, Taedok Science Town, Taejeon 305-606

(Received 9 April 1991)

A force sensor which employs the measurement of the change in the maximum induction of an amorphous core was constructed. This force sensor has a standard deviation of the non-linearity less than 0.1% within the range of 0 to 1 N, and a resolution of 1×10^{-1} N for the core cross section of 6×10^{-6} m². The sensor can also measure transient force at a sampling rate of 10 kHz which is the same as the magnetizing frequency of the core.

I. Introduction

The load cells are widely used for the measurement of force. The load cell employs different kind of principles, for example, 1) strain gauge, 2) electromagnetic force compensation, 3) vibrating-string, 4) gyroscope, 5) tuning-fork, 6) capacitive, 7) piezoelectric, and 8) magnetoelastic[1]. The magnetoelastic force sensor uses the changes of magnetic properties of magnetic material under stress. Amorphous magnetic material is suitable for this type of the force sensor because of its high yield stress and magnetoelastic properties. Highly magnetostrictive amorphous material has been applied to force sensor[2,3]. Most magnetostrictive force sensors make use of the change in the permeability as measurand[4,5]. In other case, the measurement is based on the multi-vibrator bridge technique[6,7].

Recently a new kind of force sensor was introduced [8,9], in which the measurement of the changes of the maximum induction in ac magnetization of an amorphous alloy was used. In this work, we have constructed an improved weighing machine and studied in more detail the physical characteristics of the force sensor to improve the linearity and sensitivity.

II. Construction of the sensor

For the construction of the force sensor, a Co-based amorphous ribbon ($\text{Co}_{42}\text{Ni}_{15}\text{Si}_8\text{B}_{15}$, saturation magnetostriction $\lambda_s = -6 \times 10^{-6}$) produced by vacuum schmelze, was used. The changes of hysteresis loop of this material at magnetizing frequency of 10 kHz under different tensile stresses is shown in Fig.1. From this figure, one can apply to a force sensor if the change of the maximum induction ΔB_{\max} is used as a measurand. This decrement ΔB_{\max} is approximately proportional to the tensile stress within a certain range i.e.:

$$\Delta B_{\max} = k \sigma \quad (1)$$

where σ is the tensile stress ($\sigma = F/A$; F is the external force and A is cross sectional area of the core) and k is a proportional constant which is the function of magnetizing frequency and maximum magnetic field strength.

For the development of the force sensor, we have constructed a weighing machine which uses Roberval principle as shown in Fig.2. For the core material, 2mm wide, 50mm long and $30 \mu\text{m}$ thick amorphous strip was etched from the 25.4mm wide as-quenched ribbon. A

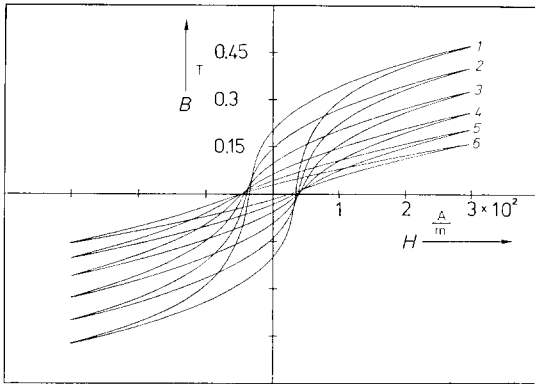


Fig. 1. The changes of hysteresis loop of $\text{Co}_{62}\text{Ni}_{15}\text{Si}_8\text{B}_{15}$ amorphous ribbon at 10 kHz under different tensile stresses (1 : $\sigma = 0 \text{ N/mm}^2$, 2 : $\sigma = 19 \text{ N/mm}^2$, 3 : 38 N/mm^2 , 4 : $\sigma = 57 \text{ N/mm}^2$, 5 : $\sigma = 76 \text{ N/mm}^2$, 6 : $\sigma = 95 \text{ N/mm}^2$).

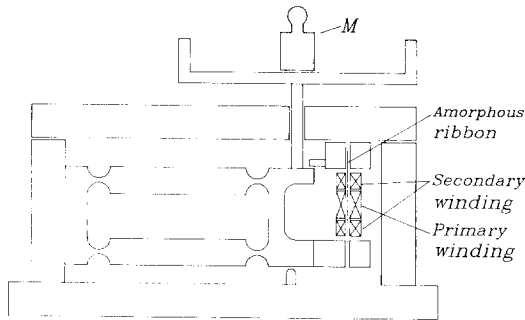


Fig. 2. Schematic diagram of the force sensor.

bakelite was used as coil former material. The magnetizing coil N_1 of 280 turns, 15 mm in length was wound using 0.14 mm ϕ enamelled copper wire at the center of the coil former. The secondary coils N_2 of 100 turns each, 5 mm in length were wound at the ends of coil former. Two secondary coils were connected in series.

The block diagram of the measuring circuit is shown in Fig.3. For the measurement of maximum magnetic induction B_{max} of the core, a quadrature oscillator(BB 4423) was used. Sinewave output of the oscillator is fed into a voltage to current converter to magnetize the core. The time position of the B_{max} is the same as that of the maximum magnetic field strength H_{max} which is proportional to the primary current. This time positions correspond to the zero crossing points of cosinewave of the oscillator and are independent of external force. To mea-

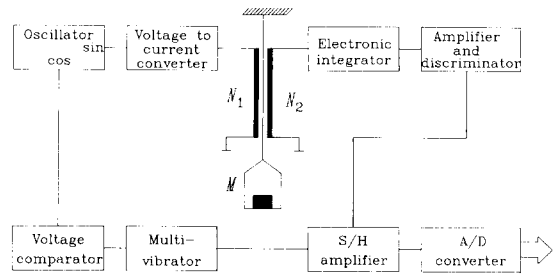


Fig. 3. Block diagram of the measuring circuit of the force sensor.

sure ΔB_{max} , the secondary voltage is integrated using Miller integrator. The integrated signal is fed into non-inverting input of instrumentation amplifier. A dc reference voltage which corresponds to the voltage is integrated using Miller integrator. The integrated signal is fed into non-inverting input of instrumentation amplifier. A dc reference voltage which corresponds to the voltage of B_{max} under zero tensile stress is fed into inverting input of the instrumentation amplifier. The output signal of the instrumentation amplifier is fed into the analog input of the sample and hold (S/H) amplifier. Sampling pulses for the S/H amplifier are obtained from the zero crossing points of the cosinewave using the voltage comparator and multivibrator.

The relation between the output voltage U_o of the S/H amplifier and the force, which is derived from equation (1), is as follows:

$$U_o = \frac{KGN_2}{RC} F \quad (2)$$

where G is amplification factor of the instrumentation amplifier and RC is time constant of the Miller integrator. From equation (2), one can see that the transfer function (U_o/F) of the force sensor, within a certain linear range for external force, is independent of the external force. Moreover, the measuring time positions are also independent of the external force. From above conditions, one can measure a transient force with a sampling rate which is the same as magnetizing frequency of the core.

III. Experimental results and discussion

The sensor output voltage (U_o) vs. force (F), in the

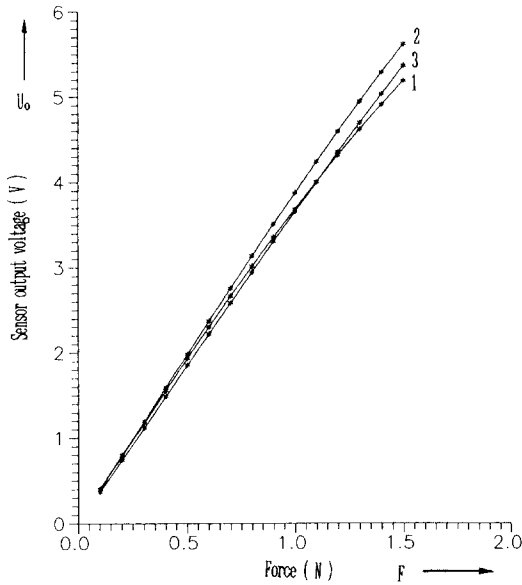


Fig. 4. Output voltage of the force sensor as a function of the external force at 10 kHz for different maximum magnetizing current I_{max} (1 : 30 mA, 2 : 60 mA, 3 : 100 mA).

range of 0 to 1.47 N for the magnetizing frequency of 10 kHz for the different maximum magnetizing current I_{max} , is shown in Fig.4. This figure shows that the linearity and sensitivity depend on the I_{max} . That means one can not find easily the optimum conditions for the linearity and sensitivity. To understand the characteristics of sensor, the output voltage vs. I_{max} at fixed magnetizing frequency f_m and the output voltage vs. f_m at fixed maximum magnetizing current I_{max} were measured. Fig.5. shows that the output voltage depends on the I_{max} under the force of 1.47 N. From this figure, one can see that the output voltage increases in the range of low magnetizing current and reaches its maximum value and then decreases slowly as the current increases. The maximum values of the sensor output voltage were obtained at $I_{max}=30$ to 40 mA with magnetizing frequency of 2 kHz, and at $I_{max}=60$ mA with the magnetizing frequency of 10 kHz. As I_{max} the maximum magnetizing current becomes higher, the voltage U_o becomes independent of magnetizing frequency. This can be interpreted from the behavior of ac hysteresis loop i.e. the maximum magnetic induction is independent of magnetizing frequency

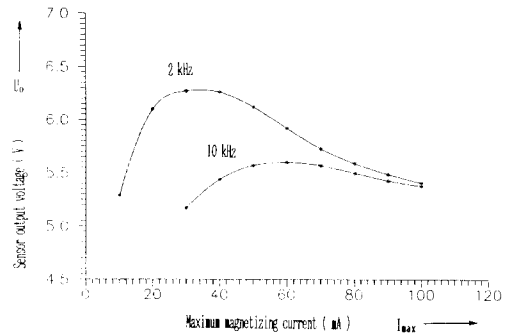


Fig. 5. Output voltage of the force sensor as a function of the maximum magnetizing current at 2 kHz and 10 kHz under the tensile stress of 1.47 N.

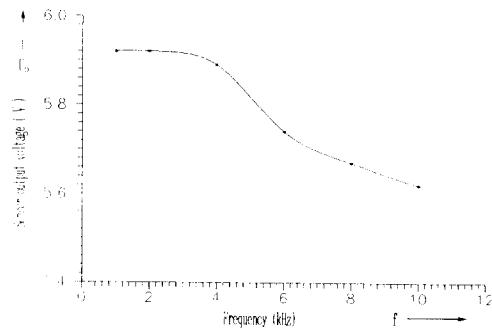


Fig. 6. Frequency dependence of the force sensor output voltage at maximum magnetizing current of 60 mA under the tensile stress of 1.47 N.

for high magnetic field strength, and peak permeability depends strongly on frequency for lower peak magnetic field strength. The frequency dependence of the sensor output voltage under the force of 1.47 N is shown in Fig.6. The voltage U_o is nearly constant up to the magnetizing frequency of 4 kHz. Between 4 kHz and 6 kHz, there is relatively large change in U_o , and above 6 kHz it decreases linearly. From Fig.5 and Fig.6, one can suggest that the higher magnetizing frequency is better for the requirement of high dynamic characteristic of the force sensor at the expense of the sensitivity and linearity. In opposite case, for higher sensitivity and linearity, the lower magnetizing frequency is better but the dynamic characteristics becomes poor. For higher magnetizing current, the effect of external magnetic field for sensor becomes smaller but sensitivity becomes lower. From above discussion, we suggest that the force

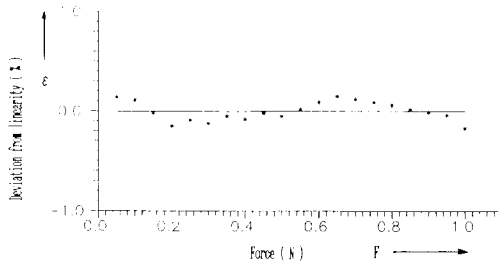


Fig. 7. Deviation from linearity ϵ of the force sensor at magnetizing frequency of 2kHz and the maximum magnetizing current of 40 mA.

sensor should be required the different conditions of magnetizing frequency and maximum magnetizing current for the purpose of application.

To demonstrate the linearity of the force sensor, the deviations from the linearity ϵ at the magnetizing frequency of 2 kHz and the maximum magnetizing current of 40 mA is shown in Fig.7. The non-linearity of the sensor was smaller than 0.1% up to 1 N and the sensitivity was better than 1×10^{-4} N. To demonstrate the dynamic characteristic of the sensor, the mechanical shock of the table was measured using a digital oscilloscope and shown in Fig.8. The magnetizing frequency and maximum magnetizing current was 10 kHz and 60 mA respectively for this measurement. The external transient force was measured at the sampling rate of 10 kHz as shown in Fig.8.

IV. Conclusion

In this work, a force sensor which employs the changes of the maximum magnetic induction of amorphous alloy was developed and tested on the various characteristics for the possible applications. The best results of the achieved linearity was 0.1% at magnetizing frequency of 2kHz and the maximum magnetizing current of 40 mA in the range of 0 to 1 N for the core cross section of $6 \times 10^{-8} \text{ m}^2$. The force sensor can measure a transient force with a sampling rate of 10 kHz which is the same as the magnetizing frequency of the core.

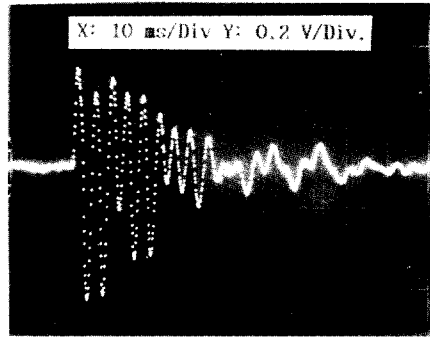


Fig. 8. Digital oscilloscope display of the force sensor output voltage under the mechanical shock of the measuring table to demonstrate the dynamical property of the sensor.

Acknowledgement

The authors wish to thank Vacuumschmelze GmbH for donating the amorphous core material. This work was supported in part by Ministry of Science and Technology, the Republic of Korea.

References

- [1] M. Kochsiek and B. Meissner, PTB-Bericht, PTB-MA-4e.
- [2] R. Boll and H. Warlimont, IEEE Trans.Mag., MAG-17, 3053-3058(1961).
- [3] K. Mohri, IEEE Trans. Mag., MAG-20, 942-947(1984).
- [4] T. Meydan and K. J. Overshott, J. Appl. Phys., 53, 8383-8385(1982).
- [5] R. Boll and G.Hinz, Tech. Messen, 52, 189-198(1985).
- [6] K. Mohri and S.Korekoda, IEEE Trans. Mag., MAG-14, 1071-1075(1978).
- [7] K. Mohri and E.Sudoh, IEEE Trans. Mag., MAG-15, 1806-1808(1979).
- [8] D. Son and J. D. Sievert, IEEE Trans. Mag., MAG-26, 2017-2019(1990).
- [9] J. Seekircher and B.Hoffmann, Sensor and Actuator, A21-A23, 401-405(1990).

비정질합금을 이용한 자기탄성 힘센서

손대락 · 김창석

한국표준연구소 자기연구실

대덕연구단지 P.O.BOX 3

(1991년 4월 9일 받음)

비정질 합금의 최대자기유도변화율 이용한 힘센서를 제작하였다. 시편의 단면적이 $6 \times 10^{-8} \text{ m}^2$ 이고 힘의 범위가 0-1N에서 힘센서의 선형도는 0.1% 이상이였으며, 분해능이 $1 \times 10^{-4} \text{ N}$ 이었다. 또한 이 힘센서는 자화주파수와 동일한 샘플링속도로 과도적인 힘을 측정할 수 있음을 보여 주었다.